Title
A conifer metabolite corrects episodic ataxia type 1 by voltage sensor—mediated ligand activation of Kv1.1

Journal
Proceedings of the National Academy of Sciences of the United States of America, 122(2)

ISSN
0027-8424

Authors
Manville, Rían W
Foglia, Lorenzo
Yoshimura, Ryan F
et al.

Publication Date
2025-01-14

DOI
10.1073/pnas.2411816122

Peer reviewed

PNAS RESEARCH ARTICLE | PHYSIOLOGY OPEN ACCESS

A conifer metabolite corrects episodic ataxia type 1 by voltage sensor-mediated ligand activation of Kv1.1

Rían W. Manville[a], Lorenzo Foglia[b], Ryan F. Yoshimura[a], Derk J. Hogenkamp[a], Amy Nguyen[a], Alvin Yu[b,1], and Geoffrey W. Abbott[a,1]

Edited by Stephen C. Cannon, University of California Los Angeles David Geffen School of Medicine, Los Angeles, CA; received June 12, 2024; accepted November 23, 2024 by Editorial Board Member Mark T. Nelson

Loss-of-function sequence variants in *KCNA1*, which encodes the voltage-gated potassium channel Kv1.1, cause Episodic Ataxia Type 1 (EA1) and epilepsy. Due to a paucity of drugs that directly rescue mutant Kv1.1 channel function, current therapeutic strategies for *KCNA1*-linked disorders involve indirect modulation of neuronal excitability. Native Americans have traditionally used conifer extracts to treat paralysis, weakness, and pain, all of which may involve altered electrical activity and/or Kv1.1 dysfunction specifically. Here, screening conifer extracts, we found that *Chamaecyparis pisifera* increases wild-type (WT) Kv1.1 activity, as does its prominent metabolite, the abietane diterpenoid pisiferic acid. Uniquely, pisiferic acid also restored function in 12/12 EA1-linked mutant Kv1.1 channels tested in vitro. Crucially, pisiferic acid (1 mg/kg) restored WT function in Kv1.1$^{E283K/+}$ mice, a model of human EA1. Experimentally validated all-atom molecular dynamics simulations in a neuron-like membrane revealed that the Kv1.1 voltage-sensing domain (VSD) also acts as a ligand-binding domain akin to those of classic ligand-gated channels; binding of pisiferic acid induces a conformational shift in the VSD that ligand-dependently opens the pore. Conifer metabolite pisiferic acid is a promising and versatile therapeutic lead for EA1 and other Kv1.1-linked disorders.

KCNA1 | potassium channel | Kv1.1 | episodic ataxia | voltage gating

Significance

Episodic ataxia type 1 (EA1) is a movement disorder caused by sequence variants in the *KCNA1* gene, which encodes the Kv1.1 potassium channel. Current therapies for EA1 do not directly rescue function of the Kv1.1. Here, we report our finding that a metabolite from a conifer tree (pisiferic acid) rescues activity of EA1-linked mutant Kv1.1 channels and also restores function in a mouse model of EA1. While Kv1.1 channels are normally activated by cell membrane depolarization, pisiferic acid binds to the Kv1.1 voltage-sensing domain, mimicking the effects of membrane depolarization to activate Kv1.1 and overcome EA1-linked dysfunction. Natural product pisiferic acid, also found in rosemary, is a promising therapeutic lead compound for EA1 and Kv1.1-linked epilepsy.

Voltage-gated potassium (Kv) channels are essential for coordinated electrical activity in the brain, peripheral nerves, muscle, and other excitable tissues. Consequently, genetic and acquired dysfunction of Kv channels causes diseases of electrical excitability. Episodic ataxia syndromes encompass a genetic and clinical spectrum of movement disorders characterized by recurring episodes of poor coordination and balance, but can also comprise blurred vision, emesis, hemiplegia, migraines, muscle weakness, myokymia, nausea, seizures, slurred speech, tinnitus, and vertigo (1, 2). Episodic ataxia 1 (EA1), an autosomal dominant inherited excitability disorder affecting balance, coordination, gait, and speech (1), is caused by sequence variants in human *KCNA1,* which encodes Kv1.1 (1, 3). EA1 is typically caused by loss-of-function variants that directly disrupt Kv1.1 gating or ion conduction (4, 5). There is a spectrum of effects on Kv1.1 in EA1—some mutants reduce current by >50% in the heterozygous state and are therefore considered dominant negative, while others impart more subtle differences (6). Because Kv1.1 is especially important for normal activity in the cerebellum, hippocampus, neocortex, synaptic terminal sites, and juxtaparanodal regions of the nodes of Ranvier of myelinated axons, EA1 disrupts both central and peripheral nerve function.

Once diagnosed, EA1 is generally treated using anticonvulsant/antiseizure drugs, including carbamazepine (7) and acetazolamide (8–10), neither of which directly fixes the function of Kv1.1 channels harboring EA1-linked variants, and which exhibit variable tolerability and efficacy. Small molecules that can directly fix EA1 mutant Kv1.1 channel function are extremely scarce, only very recently identified, and none are in clinical use for EA1. The first to be identified were gallic acid and tannic acid, which we found to improve function in vitro in EA1-linked Kv1.1-E283K and Kv1.1-L155P channels by binding to the Kv1.1 voltage sensor. We uncovered the potential use of these compounds by learning from the traditional medicine practices of the Kwakwaka'wakw First Nations, who treated ataxia with nettle, bladderwrack kelp, and Pacific ninebark, each of which contain gallic and/or tannic acid (11). Gallic acid is a promising therapeutic because it is a highly potent Kv1.1 opener and a well-tolerated over-the-counter supplement. However, it exhibited a relatively limited scope of action against a panel of EA1 sequence variants rescuing 2/5 heterozygous [wild-type (WT)/mutant] homomeric Kv1.1 channels that we tested (E283K and L155P, but not G311D, L328V, nor V408A) (11).

Here, again guided by Native American traditional medicine approaches, we explored additional plant extracts for potential therapeutic activity on Kv1.1 channels. We focused on conifers, which feature widely in Native American medicine for treatment of disorders including

Author affiliations: [a]Bioelectricity Laboratory, Department of Physiology and Biophysics, School of Medicine, University of California, Irvine, CA 92697; and [b]Department of Physiology and Biophysics, School of Medicine, University of California, Irvine, CA 92697

Author contributions: R.W.M., R.F.Y., D.J.H., A.Y., and G.W.A. designed research; R.W.M., L.F., R.F.Y., D.J.H., A.N., A.Y., and G.W.A. performed research; R.W.M., L.F., R.F.Y., D.J.H., A.N., and A.Y. analyzed data; and A.Y. and G.W.A. wrote the paper.

The authors declare no competing interest.

This article is a PNAS Direct Submission. S.C.C. is a guest editor invited by the Editorial Board.

[1]To whom correspondence may be addressed. Email: alviny6@uci.edu or abbottg@hs.uci.edu.

This article contains supporting information online at https://www.pnas.org/lookup/suppl/doi:10.1073/pnas.2411816122/-/DCSupplemental.

Published December 30, 2024.

paralysis, weakness, pain, and cardiovascular issues (12), all of which typically involve altered electrical activity and some of which involve Kv1.1 dysfunction specifically. One active conifer extract contained a compound that, remarkably, restored some or all function in 12/12 EA1 sequence variant-containing Kv1.1 channels that we tested in vitro. We also found that the compound restores WT function in vivo in a mouse model of EA1. Using all-atom molecular dynamics simulations of Kv1.1 in a model neuronal membrane followed by mutagenesis and functional analysis, we also identified and validated the small molecule binding site and mechanism of action.

Results

Screening of Conifer Needle Extracts Reveals WT Kv1.1 Channel Openers. We collected and methanol-extracted needle and twig samples from *Pinus contorta* (lodgepole pine; two separate samples), *Tsuga mertensiana* (mountain hemlock), *Pinus albicaulis* (whitebark pine), and *Pinus ponderosa* (ponderosa pine) collected from Yosemite National Park (CA) and from commercially sourced *Chamaecyparis pisifera* (Sawara or False Cypress), which is native to Japan (Fig. 1 *A* and *B*). We studied the effects of 2% extracts (5 mg solid starting material per mL) of the conifers on WT human Kv1.1 expressed in *Xenopus* oocytes, using two-electrode voltage-clamp. All extracts altered the functional properties of Kv1.1 (Fig. 1*C*). All but one (*P. albicaulis*) negative-shifted the midpoint voltage dependence of Kv1.1 activation ($V_{0.5act}$) (Fig. 1*D*), which increases channel activity at negative membrane potentials, generally a beneficial property when attempting to correct the effects of Kv channel loss-of-function sequence variants (13). Increased Kv1.1 channel activity dampens neuronal excitability, while loss-of-function mutations in Kv1.1, such as those in EA1, have the opposite effect, pathologically increasing action potential generation, firing frequency, action potential duration, and neurotransmitter release (14). All extracts hyperpolarized the E_M of oocytes expressing Kv1.1, the smallest effect being for *P. albicaulis* (Fig. 1*E*), correlating with its minimal effects on $V_{0.5act}$ and diminishment of peak current (Fig. 1*D*).

The traces (Fig. 1*C*) indicated that all but *C. pisifera* diminished Kv1.1 peak current and/or slowed activation, despite left-shifting $V_{0.5act}$ in most cases, and this was borne out by quantitative analysis (Fig. 2 *A* and *B*). All Kv channels form as tetramers of pore-forming α subunits, and many can and do form heteromeric channels in vitro and in vivo, generally with isoforms of the same subfamily (15). Kv1.1 can form functional homomeric channels in vitro, but in native neurons is thought to occur exclusively in heteromers with same-subfamily α subunits, especially Kv1.2 (except in certain disease states, e.g., multiple sclerosis, where homomeric Kv1.1 is thought to be expressed on the surface of demyelinated neurons) (16–18). Importantly, efficient neuromuscular transmission requires normal function of Kv1.1/Kv1.2 channels at juxtaparanodal regions and branch points of myelinated axons (18–22). Therefore, we also tested effects on channels containing Kv1.2. We found that both *C. pisifera* and *P. ponderosa* extracts left-shifted homomeric Kv1.2 $V_{0.5act}$ and hyperpolarized E_M of homomeric Kv1.2-expressing oocytes (Fig. 2 *C*–*E*). *C. pisifera* extract also left-shifted Kv1.1/Kv1.2 heteromer $V_{0.5act}$ and hyperpolarized the E_M of Kv1.1/Kv1.2-expressing oocytes (Fig. 2 *F*–*H*). Crucially, *C. pisifera* extract left-shifted $V_{0.5act}$ in "heterozygous" mimic channels generated by coexpression of 1:1 WT and EA1-linked V408A Kv1.1, restoring WT voltage dependence, and hyperpolarized the E_M of oocytes expressing this mutant channel (Fig. 2 *I*–*K*). The unique combination of not slowing the activation rate of Kv1.1, not reducing the peak current of Kv1.1, and of left-shifting $V_{0.5act}$ of Kv1.1, Kv1.2, Kv1.1/Kv1.2, and Kv1.1/Kv1.1-V408A [which we previously found gallic acid could not do (11)], identified *C. pisifera* as the most promising extract for further study.

Identification of Pisiferic Acid as an Efficacious and Versatile Opener of WT and EA1-Linked Mutant Kv1.1. Previous analyses of conifer extracts showed that pisiferic acid is a primary component of *C. pisifera* that is lacking in extracts from the other conifers we studied (23–29). Here, we confirmed the presence of pisiferic acid in our *C. pisifera* extract using high-performance liquid chromatography (HPLC) and liquid chromatography/mass spectrometry (LC/MS) (*SI Appendix*, Fig. S1). Interestingly, we previously found that pisiferic acid is ineffective at opening KCNQ potassium channels (30). Here, application of pisiferic acid (10 μM) in bath solution to WT human Kv1.1 expressed in oocytes robustly increased its current (e.g., 19-fold at −40 mV) (Fig. 3 *A* and *B*) by negative-shifting the $V_{0.5act}$ by −19 mV (increasing to a −38 mV hyperpolarization at 100 μM) (Fig. 3 *C* and *D*), which led to a robust hyperpolarization of E_M (Fig. 3*E*). Dose–response studies revealed that the EC_{50} for negative-shifting the Kv1.1 $V_{0.5act}$ was 12 μM, and for shifting the E_M of Kv1.1-expressing oocytes was 9 μM pisiferic acid (reaching >−30 mV hyperpolarization at 100 μM) (Fig. 3 *F* and *G*). Pisiferic acid did not alter Kv1.1 activation rate (Fig. 3*H*), but decreased Kv1.1 deactivation rate >sixfold, consistent with pisiferic acid stabilizing the Kv1.1 open state (Fig. 3*I*). Kv1.1 channels did, however, still close in the presence of pisiferic acid (*SI Appendix*, Fig. S2).

As described above, Kv1.1 forms complexes with Kv1.2 in vivo. Here, we found that pisiferic acid (10 μM) was also effective at increasing Kv1.2 currents (Fig. 3 *J* and *K*), negative-shifting the $V_{0.5act}$ by −13 mV (Fig. 3 *L* and *M*) and hyperpolarizing E_M by −17 mV (Fig. 3*N*). Dose–response studies revealed the EC_{50} for negative-shifting the Kv1.2 $V_{0.5act}$ was 13 μM, and for shifting the E_M of Kv1.1-expressing oocytes was 9 μM pisiferic acid (Fig. 3 *O* and *P*). Pisiferic acid (12 μM) also negative-shifted $V_{0.5act}$ of heteromeric Kv1.1/Kv1.2 channels (by −14 mV) (Fig. 3 *R* and *S*) and hyperpolarized E_M of oocytes expressing Kv1.1/Kv1.2 by −19 mV (Fig. 3*T*).

Thus, pisiferic acid is an opener of both Kv1.1 and Kv1.2, whereas we previously found it does not activate KCNQ channels (30). Here, we also found that pisiferic acid (12 μM) has negligible effects on Kv2.1 and on hERG (*SI Appendix*, Fig. S3). A recent report showed that niflumic acid is also a Kv1.1 opener, with a reported EC_{50} of 272 μM (31), less potent than pisiferic acid (32–34). We directly compared the effects of niflumic acid and observed EC_{50} values of 347 and 120 μM, for negative-shifting Kv1.1 $V_{0.5act}$ and hyperpolarizing E_M of Kv1.1-expressing oocytes, respectively, similar to the previous report (31) and demonstrating that pisiferic acid is a 29-fold more potent opener of Kv1.1 than niflumic acid (*SI Appendix*, Fig. S4*A*). We previously found that gallic acid opens Kv1.1 with an EC_{50} of 0.54 μM, making it 22-fold more potent than pisiferic acid (30). While gallic acid was the first reported small molecule opener of Kv1.1 channels harboring EA1-linked loss-of-function variants, it is not a broad-spectrum opener of Kv1.1 channels carrying pathogenic sequence variants, rescuing 2/5 tested (E283K and L155P, but not G311D, L328V, nor V408A) (30). Niflumic acid was previously shown to rescue Kv1.1-V408A function but data for other sequence variants were not shown (31). Therefore, here we tested effects of pisiferic acid on 12 different pathogenic Kv1.1 sequence variants spanning all transmembrane segments and the N-terminal domain L155P variant we reported previously (35) (*SI Appendix*, Fig. S4*B*).

We first tested homomeric, homozygous EA1-mutant Kv1.1 channels, generated by expressing only mutant Kv1.1 channel subunits, which exhibit the most severe defects in vitro but are highly unlikely to exist in vivo because Kv1.1 heteromerizes with e.g., Kv1.2 in vivo and EA1 is an autosomal dominant disorder. At its EC_{50} (12 μM), pisiferic acid restored some or all

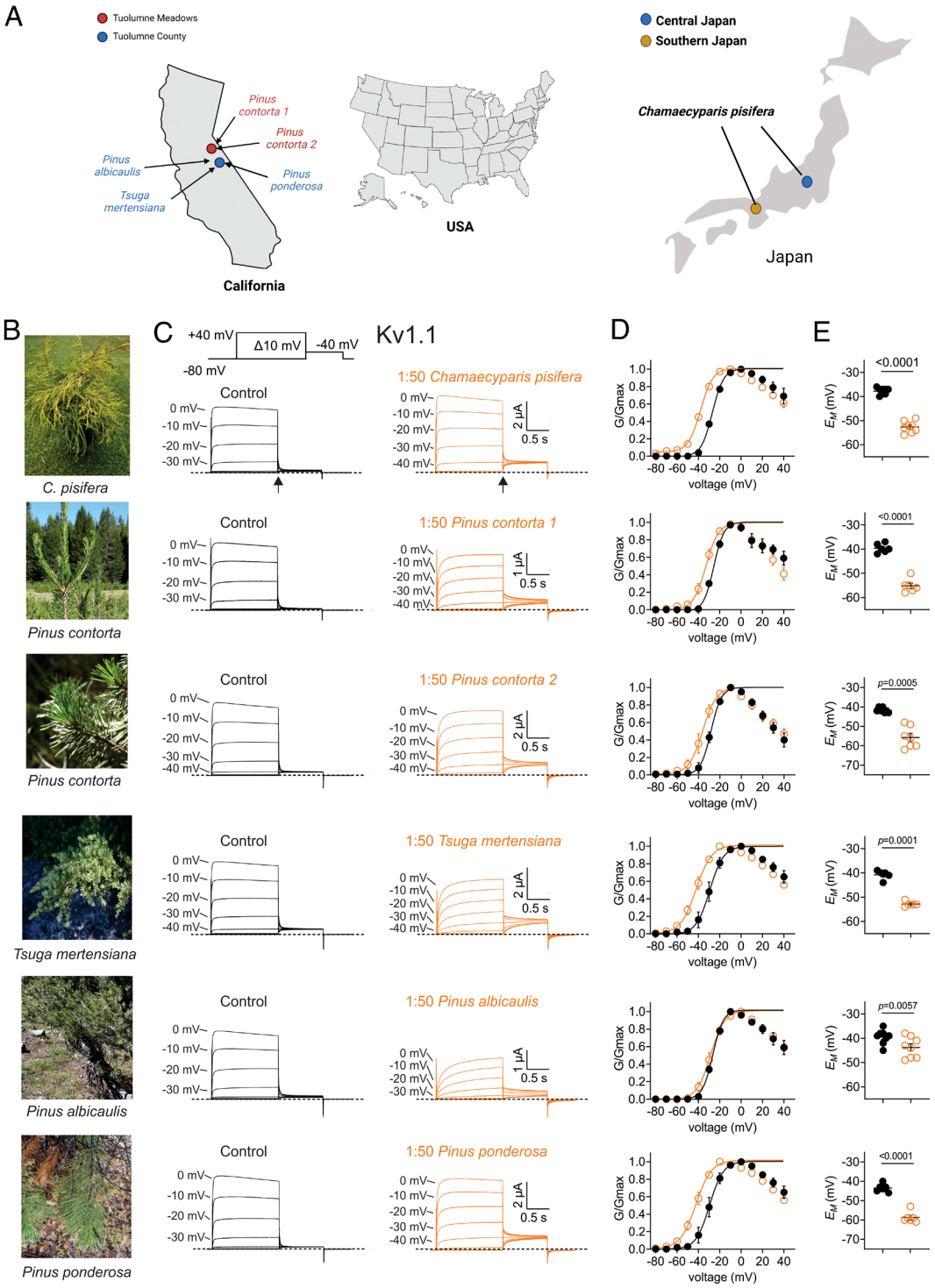

Fig. 1. Conifer extract screening for Kv1.1 opening activity. Error bars indicate SEM. *n* indicates number of biologically independent oocytes. At least 2 batches of oocytes were used per experiment. Statistical comparisons by the two-tailed paired *t* test. Dashed lines indicate zero current line here and throughout. (*A*) Geographical location of wild sources of Californian conifer samples (*Left*) and native range of commercially sourced *C. pisifera* (*Right*). Maps created with BioRender.com. (*B*) Conifers from which samples were taken for analysis. Photos taken by senior author (GWA). (*C*) Mean traces for Kv1.1 expressed in oocytes in the absence (Control) or presence of 1:50 dilution conifer extracts as indicated. Scale bars *Upper Right* for each pair of traces; voltage protocol *Upper Left Inset*; *n* = 5-8 per group. Arrows indicate where tail current measurements are made for G/Gmax plots. (*D*) Mean normalized tail current (G/Gmax) for traces as in (*C*); *n* = 5-8 per group. (*E*) Mean unclamped oocyte membrane potential for oocytes as in (*C*); *n* = 5-8 per group.

function in homomeric, homozygous R167M, E283K, F303V, R324T, I407M, and V408A channels, increasing their activity (*SI Appendix*, Fig. S4*C*), negative-shifting their voltage dependence of activation (*SI Appendix*, Fig. S4*D*), and hyperpolarizing the E_M of oocytes expressing them (*SI Appendix*, Fig. S4*E*). In contrast, pisiferic acid was unable to rescue homomeric, homozygous L155P, T226K, N255K, R307C, G311D, or L319R mutant channels (*SI Appendix*, Fig. S5). Homozygous, homomeric rescues are colored green in *SI Appendix*, Fig. S4*B*; nonrescues are colored orange.

We next studied effects on channels formed by coinjection in oocytes of 50% WT Kv1.1 cRNA and 50% EA1-mutant Kv1.1 cRNA, to mimic in a reductionist system the heterozygous status of individuals with EA1. As Kv channels are tetrameric, this is expected to produce a mix of channels, including all-WT, all-mutant, and channels with 1 to 3 mutant or WT subunits. This is a standard reductionist approach to approximating autosomal dominant disease states in vitro. Strikingly, pisiferic acid (12 µM) was able to improve function (*SI Appendix*, Fig. S6*A*) and restore voltage dependence similar to or more responsive than WT Kv1.1 (*SI Appendix*, Fig. S6*B*) in 11/12 EA1 mutants tested, the exception being R307C which was completely nonfunctional with or without pisiferic acid (*SI Appendix*, Figs. S6*C* and S7) (*SI Appendix*, Fig. S6*D*). Heterozygous EA1-linked mutations reduced peak current at −20 or −30 mV by 30 to 98% (*SI Appendix*, Fig. S6*E*); pisiferic acid (12 µM) increased heterozygous,

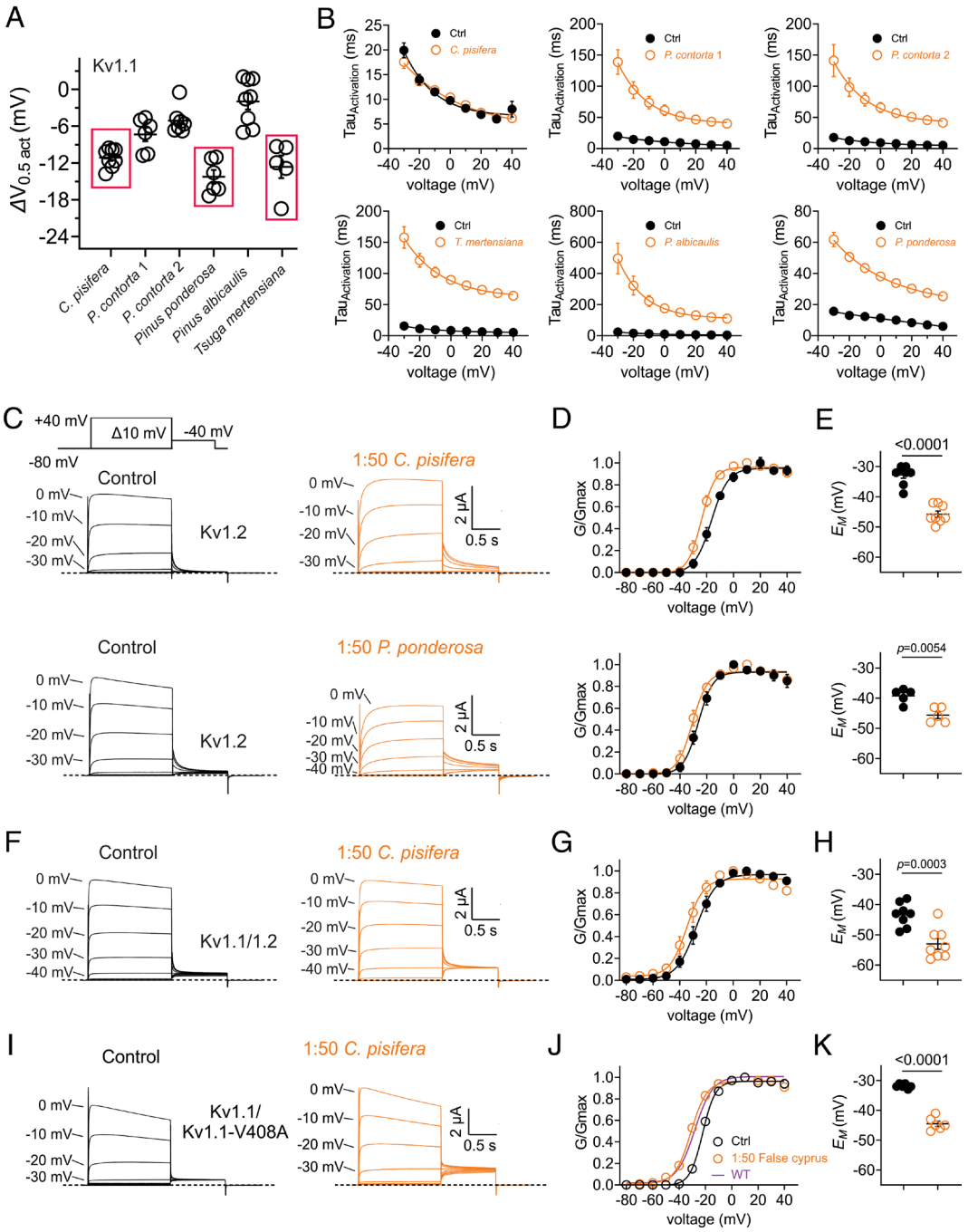

Fig. 2. Selection of optimal conifer extract for Kv1.1 activation. Error bars indicate SEM. *n* indicates number of biologically independent oocytes. At least 2 batches of oocytes were used per experiment. Statistical comparisons by the two-tailed paired *t* test. (*A*) Shift in midpoint voltage dependence of activation ($V_{0.5act}$) induced by 1/50 conifer extracts from Fig. 1, analyzed from recordings as in Fig. 1. (*B*) Shifts in activation rates induced by 1/50 conifer extracts from Fig. 1, analyzed from recordings as in Fig. 1. (*C*) Mean traces for Kv1.2 expressed in oocytes in the absence (Control) or presence of conifer extracts indicated (1/50 dilution). Scale bars *Upper Right* for each trace; voltage protocol *Upper Inset*; *n* = 5-8 per group. (*D*) Mean normalized tail current (G/Gmax) for traces as in (*C*); *n* = 5-8 per group. (*E*) Mean unclamped oocyte membrane potential for oocytes as in (*C*); *n* = 5-8 per group. (*F*) Mean traces for Kv1.1/Kv1.2 heteromers expressed in oocytes in the absence (Control) or presence of *C. pisifera* extract (1/50 dilution). Scale bars *Upper Right* for each trace; *n* = 8 per group. (*G*) Mean normalized tail current (G/Gmax) for traces as in (*F*); *n* = 8 per group. (*H*) Mean unclamped oocyte membrane potential for oocytes as in (*F*); *n* = 8 per group. (*I*) Mean traces for homomeric, heterozygous Kv1.1/Kv1.1-V408A channels expressed in oocytes in the absence (Control) or presence of *C. pisifera* extract (1/50 dilution). Scale bars *Upper Right* for each trace; *n* = 6 per group. (*J*) Mean normalized tail current (G/Gmax) for traces as in (*I*); *n* = 6 per group. (*K*) Mean unclamped oocyte membrane potential for oocytes as in (*I*); *n* = 6 per group.

homomeric mutant Kv1.1 channel current at −20 or −30 mV 2- to 10-fold (*SI Appendix*, Fig. S6*F*). While heterozygous EA1 mutations positive-shifted Kv1.1 $V_{0.5act}$ by as much as +23 mV (where possible to test) (*SI Appendix*, Fig. S6*G*), pisiferic acid (12 μM) negative-shifted Kv1.1 $V_{0.5act}$ by as much as −23 mV (*SI Appendix*, Fig. S6*H*).

As examples, the EA1 mutant G311D is in the Kv1.1 S4-5 linker (*SI Appendix*, Fig. S6*D*); it reduces prepulse current by >40% in Kv1.1/Kv1.1-G311D channels (*SI Appendix*, Fig. S6*E*); pisiferic acid increased its peak current twofold and negative-shifted its $V_{0.5act}$ by −8 mV in heteromeric channels (*SI Appendix*, Figs. S6 *F* and *H* and S7). EA1 mutant V408A is at the Kv1.1 S6 intracellular-proximal

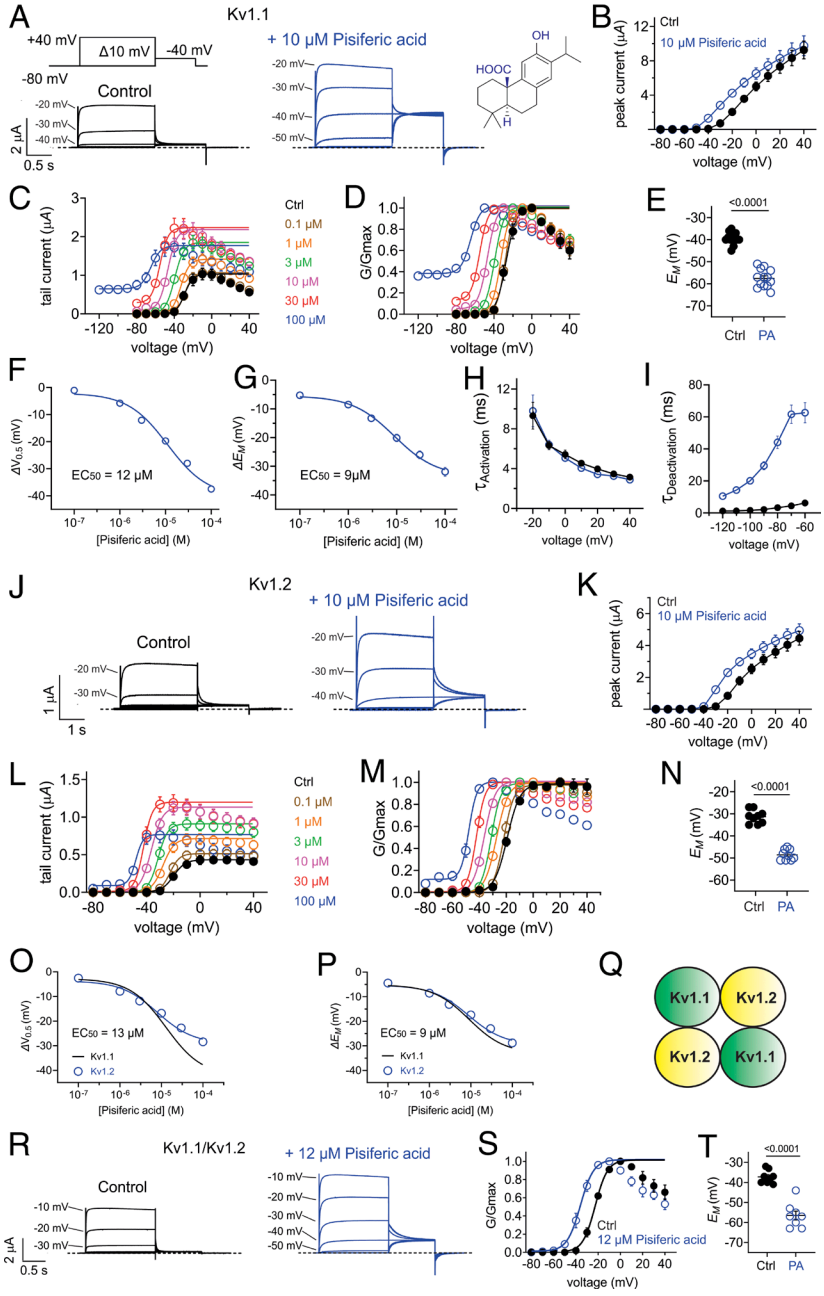

Fig. 3. *C. pisifera* metabolite pisiferic acid activates homomeric and heteromeric WT Kv1.1 and Kv1.2 channels. Error bars indicate SEM. *n* indicates number of biologically independent oocytes. At least 2 batches of oocytes were used per experiment. Statistical comparisons by the two-tailed paired *t* test. (*A*) Mean traces for Kv1.1 expressed in oocytes in the absence (Control) or presence of pisiferic acid (10 μM; structure shown in *Upper Right Inset*). Scale bars *Lower Left*; voltage protocol *Upper Left Inset* applies to all recordings in this figure; *n* = 13 per group. (*B*) Mean peak prepulse current for traces as in panel (*A*); *n* = 13 per group. (*C*) Mean tail current versus prepulse voltage using voltage protocol as in (*A*), for Kv1.1 in the absence or presence of pisiferic acid at concentrations indicated; *n* = 8 per group. (*D*) Mean normalized tail current (G/Gmax) versus prepulse voltage using voltage protocol as in (*A*), for Kv1.1 in the absence or presence of pisiferic acid at concentrations indicated; *n* = 8 per group. (*E*) Mean unclamped oocyte membrane potential for oocytes as in (*A*); *n* = 13 per group. (*F*) Shift in $V_{0.5act}$ versus [pisiferic acid] for Kv1.1 channels, recorded as in (*C*); *n* = 8 per group. (*G*) Shift in E_M versus [pisiferic acid] for Kv1.1 channels, recorded as in (*C*); *n* = 8 per group. (*H*) Activation rate ($T_{activation}$) versus voltage for Kv1.1 in the absence (black) or presence (blue) of pisiferic acid (12 μM), recorded from traces as in (*A*); *n* = 8 per group. (*I*) Deactivation rate ($T_{deactivation}$) versus voltage for Kv1.1 in the absence (black) or presence (blue) of pisiferic acid (12 μM); *n* = 6 per group. (*J*) Mean traces for Kv1.2 expressed in oocytes in the absence (Control) or presence of pisiferic acid (10 μM). Scale bars *Lower Left*; *n* = 9 per group. (*K*) Mean peak prepulse Kv1.2 current for traces as in panel (*J*); *n* = 9 per group. (*L*) Mean Kv1.2 tail current versus prepulse voltage, in the absence or presence of pisiferic acid at concentrations indicated; *n* = 6-7 per group. (*M*) Mean Kv1.2 normalized tail current (G/Gmax) versus prepulse voltage, in the absence or presence of pisiferic acid at concentrations indicated; *n* = 6 per group. (*N*) Mean unclamped oocyte membrane potential for oocytes as in (*J*); *n* = 9 per group. (*O*) Shift in $V_{0.5act}$ versus [pisiferic acid] for Kv1.2 channels; *n* = 6-7 per group. (*P*) Shift in E_M versus [pisiferic acid] for Kv1.2 channels; *n* = 6-7 per group. (*Q*) Cartoon representation of one possible subunit composition of heteromeric Kv1.1/Kv1.2 channels studied in panels (*R–T*). (*R*) Mean traces for Kv1.1/Kv1.2 heteromers expressed in oocytes in the absence (Control) or presence of pisiferic acid (12 μM). Scale bars *Lower Left*; *n* = 8 per group. (*S*) Mean Kv1.1/Kv1.2 normalized tail current (G/Gmax) versus prepulse voltage for traces as in (*R*); *n* = 8 per group. (*T*) Mean unclamped oocyte membrane potential for oocytes as in (*R*); *n* = 8 per group.

end (*SI Appendix*, Fig. S6*D*) and reduces peak current by >80%, speeds deactivation, and increases C-type inactivation of Kv1.1 (20, 36). Pisiferic acid (12 μM) doubled heterozygous, homomeric Kv1.1-V408A current at 0 mV and increased current 10-fold at −30 mV (*SI Appendix*, Fig. S6 *A* and *F*). Heterozygous, homomeric current rescues are colored green in *SI Appendix*, Fig. S6*D*; nonrescues are colored orange.

Last, we studied the effects of pisiferic acid on channels generated by coinjection of a 1:1:2 ratio of cRNA for mutant Kv1.1, WT Kv1.1, and WT Kv1.2, respectively, to approximate the heterozygous, heteromeric (Kv1.1/Kv1.2) current (generated by a mix of channel types according to the nuances of subunit assembly for each mutant) thought to occur in vivo in typical individuals with EA1. Pisiferic acid (12 μM) was able to increase channel peak current and restore voltage dependence similar to or more responsive than WT Kv1.1/Kv1.2 heteromeric channels in 12/12 EA1 mutants tested (Fig. 4 *A* and *B* and *SI Appendix*, Fig. S8), leading to hyperpolarization of E_M in all cases (Fig. 4*C* and *SI Appendix*, Fig. S8). Pisiferic acid universally restored some or all function in all EA1 mutants tested in the heterozygous, heteromeric form (Fig. 4 *D–H*).

Pisiferic Acid Corrects Episodic Ataxia Type 1 in a Mouse Model. To further test the therapeutic potential of pisiferic acid, we first used CRISPR-Cas9 to generate a new mouse model of EA1, the Kv1.1-E283K mouse line, harboring one of the 12 EA1 Kv1.1 variants we found to be responsive to pisiferic acid in vitro (*SI Appendix*, Figs. S4–S8 and Fig. 4). E283K was originally identified in an individual with paroxysmal ataxia and myokymia aggravated by painful muscular contractures of the face and limbs and metabolic dysfunction; other family members exhibited similar symptoms (18), and EA1-linked symptoms were triggered by exercise, emotional stress, and certain foods. We found that E283K was homozygous lethal in mice, consistent with another EA1 mutant mouse line (V408A) (36). We also found using LC/MS that pisiferic acid is able to cross the blood–brain barrier (BBB) after IP injection, supporting the possibility of

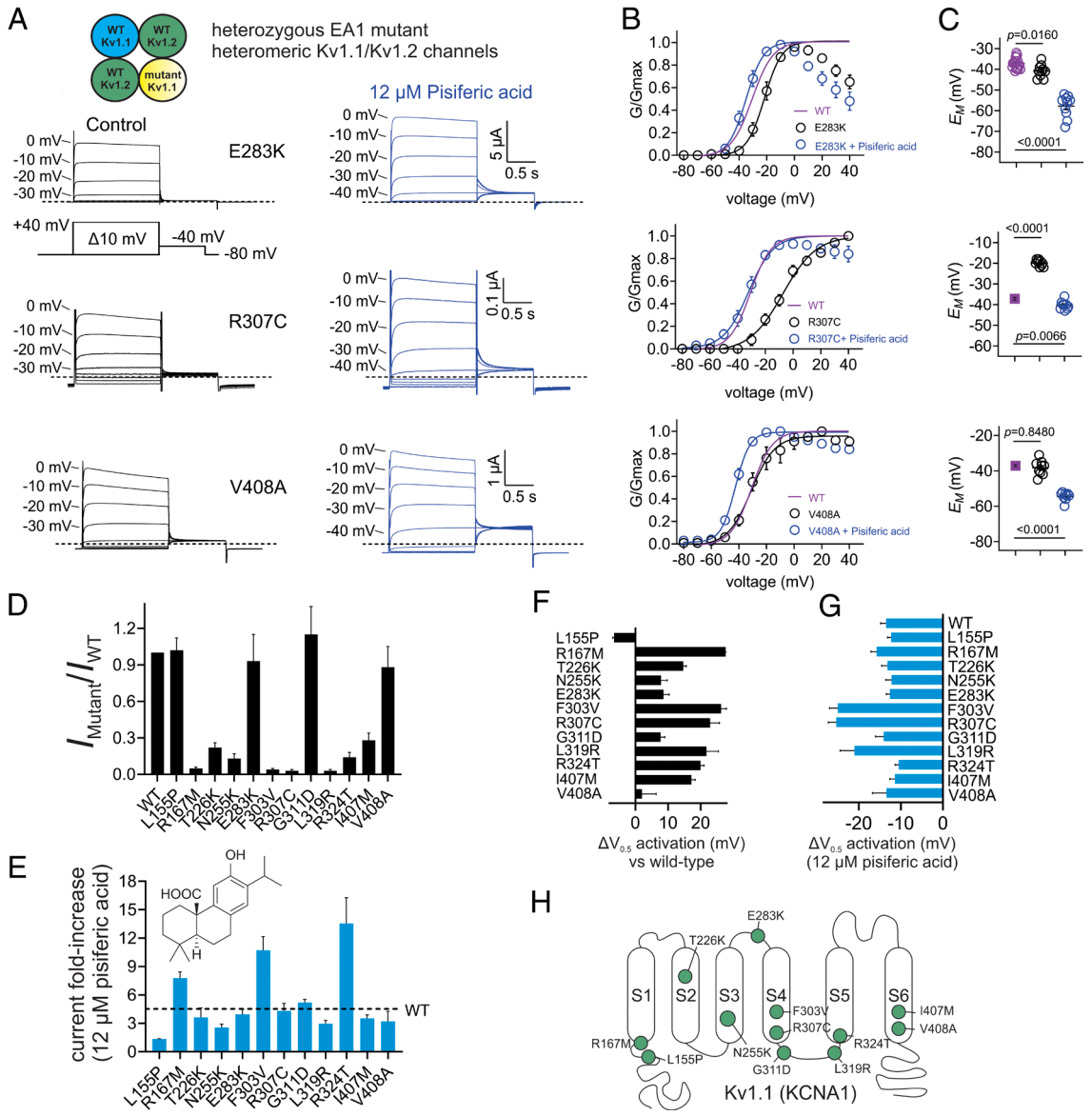

Fig. 4. Pisiferic acid improves function in 12/12 EA1 mutant heteromeric, heterozygous Kv1.1/Kv1.2 channels tested. Error bars indicate SEM. *n* indicates number of biologically independent oocytes. At least 2 batches of oocytes were used per experiment. Statistical comparisons by the two-tailed paired *t* test. (*A*) Mean traces for heteromeric, heterozygous EA1 mutant Kv1.1/Kv1.2 channels (schematic of one possible subunit composition, *Upper Left Inset*) expressed in oocytes in the absence (Control) or presence of pisiferic acid (12 μM). Scale bars *Upper Right*; voltage protocol *Left Inset*; *n* = 9-10 per group. (*B*) Mean normalized tail current (G/Gmax) versus prepulse voltage for traces as in (*A*), in the absence or presence of pisiferic acid (12 μM); *n* = 9-10 per group. (*C*) Mean unclamped oocyte membrane potential for oocytes as in a versus untreated WT; *n* = 9-10 per group. Magenta bars indicate where WT mean data were taken from panels above in cases where recordings were conducted in the same date ranges; *n* = 18. (*D*) EA1 mutant heteromeric, heterozygous Kv1.1/Kv1.2 channel peak current at −20 or −30 mV normalized to WT Kv1.1/Kv1.2 current for mutants indicated, recorded using voltage protocol shown in panel (*A*); *n* = 6-13 per group. (*E*) Current fold-increase at −20 or −30 mV induced by 12 μM pisiferic acid for EA1 mutant heteromeric, heterozygous Kv1.1/Kv1.2 channels indicated, recorded using voltage protocol shown in panel (*A*); *n* = 6-13 per group. Dashed line, 12 μM pisiferic acid-induced fold-increase in WT Kv1.1/Kv1.2 current. (*F*) Shift in $V_{0.5act}$ compared to WT Kv1.1/Kv1.2 for EA1 mutant heteromeric, heterozygous Kv1.1 channels, recorded using voltage protocol shown in panel (*A*); *n* = 6-13 per group. (*G*) Shift in $V_{0.5act}$ induced by 12 μM pisiferic acid for EA1 mutant heteromeric, heterozygous Kv1.1/Kv1.2 channels indicated, recorded using voltage protocol shown in panel (*A*); *n* = 6-13 per group. (*H*) Topology schematic of Kv1.1 showing locations of EA1 mutations studied in this project. Green, mutations for which pisiferic acid (12 μM) partially or fully corrected function in heteromeric, heterozygous Kv1.1/Kv1.2 channels.

its therapeutic utility in neurological disorders that require small molecule access to the brain (*SI Appendix*, Fig. S9).

We first tested performance on an accelerating rotarod to introduce exercise stress and found that heterozygous mutant ($Kv1.1^{E283K/+}$) mice performed worse than WT ($Kv1.1^{+/+}$) mice, the former falling on average 30 s earlier than the latter (t = 2.223, df=17, $P = 0.04$; n = 8-11 per group) (Fig. 5*A*). In contrast, when both sets of mice were pretreated with intraperitoneal (IP) injection of pisiferic acid (1 mg/kg), both sets of mice performed similarly to untreated $Kv1.1^{+/+}$ mice (t = 0.7009, df = 28, $P = 0.489$ by the unpaired *t* test; n = 10-20 per group (Fig. 5*B*).

We next induced stress using IP injections of isoproterenol (5 mg/kg) and then tested mouse performance on a balance beam. During baseline testing in the absence of isoproterenol, mice were able to cross the beam with minimal slips, regardless of genotype (t = 0.9453, df = 35, $P = 0.351$ by the unpaired *t* test; n = 15-22 per group) (Fig. 5*C* and Movies S1 and S2). After isoproterenol injections, mice slipped more frequently, and $Kv1.1^{E283K/+}$ mice slipped more than twice as often on average as $Kv1.1^{+/+}$ mice (defined as hindfoot slips reaching below the beam, scored by a blinded scorer) (Fig. 5*D* and Movies S3 and S4). Strikingly, when mice were pretreated with pisiferic acid (1 mg/kg) before

isoproterenol injections, both Kv1.1$^{+/+}$ and Kv1.1$^{E283K/+}$ mice slipped a similar number of times to untreated Kv1.1$^{+/+}$ mice (Fig. 5*D* and Movies S5 and S6). A two-way ANOVA showed a statistically significant interaction between the effects of genotype and treatment on the number of hindfoot missteps after isoproterenol challenge ($F_{1,33}$ = 4.207, P = 0.0483; n = 7-11 per group). The Bonferroni post test showed a main effect where Kv1.1$^{E283K/+}$ mice treated with 1 mg/kg pisiferic acid had a statistically significant reduction in the number of hindfoot missteps when compared to those treated with vehicle (P = 0.025). Thus, pisiferic acid (1 mg/kg) eliminates ataxia in Kv1.1$^{E283K/+}$ mice, a model of human EA1.

All-Atom Molecular Dynamics Simulations of Pisiferic Acid and Kv1.1. We previously found that gallic acid enhances Kv1.1 but not Kv1.2 activity, and used this to identify residues in S1, within the voltage-sensing domain (VSD) unique to Kv1.1 and not Kv1.2 that formed the gallic acid binding site (Fig. 6 *A* and *B*) (11). Here, we found that unlike gallic acid (11), pisiferic acid was able to negative-shift the voltage dependence of Kv1.1 carrying a triple mutant that disrupts the gallic acid binding site (Fig. 6 *C*–*F*). Thus. pisiferic acid does not share a common binding site with gallic acid.

To assess the molecular processes by which pisiferic acid activates the Kv1.1 channel, we next performed unbiased all-atom molecular dynamics (MD) simulations of the Kv1.1 channel embedded in a phospholipid bilayer with explicit solvent. The atomic model of the tetrameric channel was generated using AlphaFold (37) and structural alignment of the pore helices to the X-ray crystallographic structure of Kv1.2 (PDB ID: 2A79) (38) (Fig. 7 *A* and *B*; see *SI Appendix*, *Methods* for a complete description). Similar to prior studies of ligand binding (39–42), pisiferic acid ligands were placed into the bulk solution at least 10 Å from any nonligand molecules (Fig. 7 *C*–*F*). Three systems were prepared and selected for longer timescale simulations. In aggregate our molecular dynamics data totaled 0.9 μs. Strikingly, pisiferic acid spontaneously bound to the VSD of Kv1.1.

Molecular Mechanism of Pisiferic Acid Binding to Kv1.1. The Kv1.1 VSD contains a solvent-exposed cavity between the S1 and S4 helices, separated by approximately 17 Å between the C_α atoms of L288 and K193 (Fig. 8*A*). In the simulations, pisiferic acid enters the VSD through the cavity between the S1 and S4 helices and initially contacts E283 and Q284 on S4 (Fig. 8*B* and Movies S7 and S8). Several transient interactions form between the β-hairpin connecting the S1 and S2 helices and pisiferic acid, as well as between the S3 and S4 loop and pisiferic acid (Fig. 8 *C* and *D*). These transient contacts between the S1 and S2 β-hairpin break as the ligand then shifts into the cavity to form a CH–π interaction between L291 and the aromatic ring of pisiferic acid (Fig. 8*E*). As the β-hairpin returns to the conformation adopted prior to binding, pisiferic acid coordinates residues on the S4 helix, stabilized by interactions with the ligand's hydroxyl group interactions with the amino group of the peptide backbone of Q284 and a CH–π interaction with L291 (Fig. 8*F*). The CH–π interaction breaks as pisiferic acid rotates to contact residues K193 and E187 on the S1 helix in a metastable configuration (Fig. 8*G*). The pisiferic acid ligand then inverts and shifts deeper into the VSD (Fig. 8 *H* and *I*) eventually adopting a stable pose (Fig. 8*J*) with the hydroxyl end of the ligand forming contacts with the R295 amino acid backbone, the base of the ligand interacting with R298, which forms a salt bridge interaction with E187, and the carboxyl end of the ligand contacting R292 and K193. After binding, the C_α distance between residues L288 and K193 reduces to 12 Å reflecting a more compact VSD (Fig. 8 *K* and *L*).

The resting conformation of the Kv1.1 VSD could be significantly different than that predicted by AlphaFold. To assess this, we performed additional MD simulations of Kv1.1 in the presence

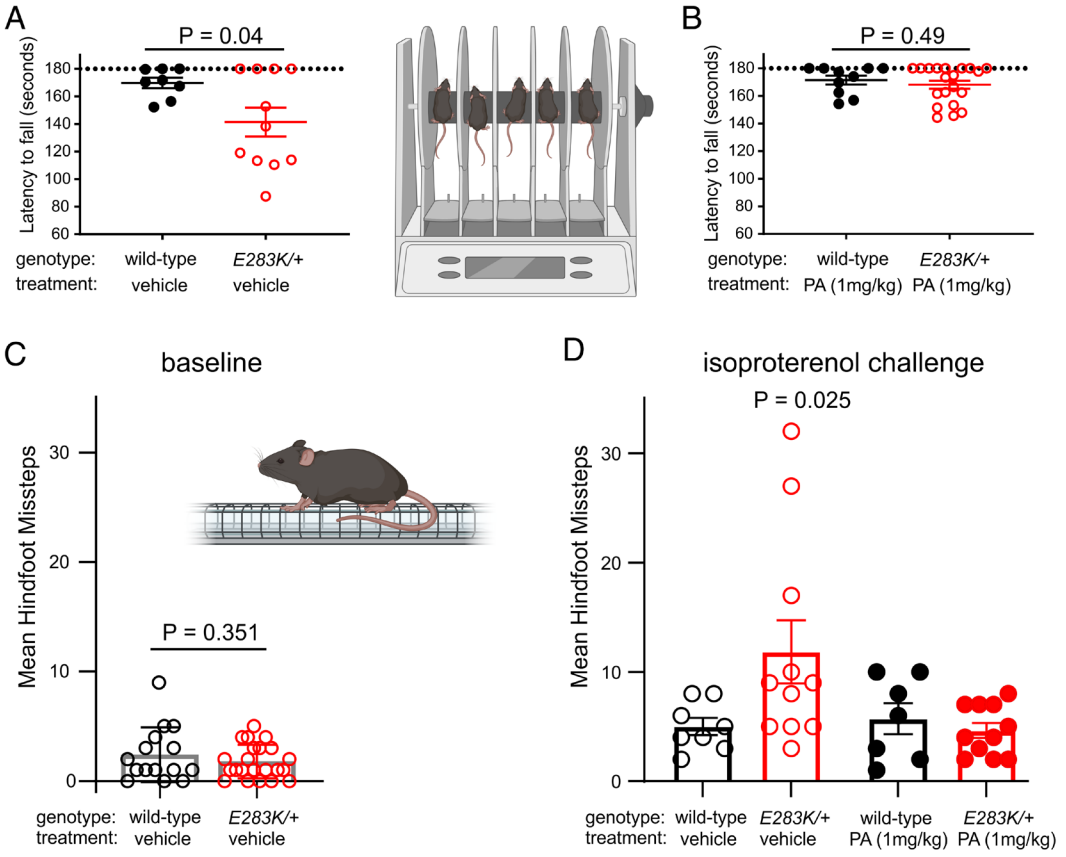

Fig. 5. Pisiferic acid restores normal function in vivo in a mouse model of human Episodic Ataxia 1. (*A* and *B*) *Kcna1*-E283K mouse performance in an accelerating rotarod paradigm. (*A*) *Kcna1*$^{E283K/+}$ mice fell from the rotarod (cartoon, *Right Inset*) significantly earlier than their WT *Kcna1*$^{+/+}$ counterparts (t = 2.223, df = 17, P = 0.0401; n = 8-11 per group). (*B*) When treated with 1 mg/kg pisiferic acid, there was no longer a statistically significant difference between *Kcna1*$^{E283K/+}$ and *Kcna1*$^{+/+}$ mice (t = 0.7009, df = 28, P = 0.4891; n = 10-20 per group). (*C* and *D*) *Kcna1*-E283K mouse performance in a balance beam paradigm. (*C*) Prior to isoproterenol challenge, there was no difference in the number of hindfoot missteps while crossing the balance beam (cartoon, *Upper Right Inset*) between *Kcna1*$^{E283K/+}$ mice and their WT *Kcna1*$^{+/+}$ counterparts (t = 0.9453, df = 35, P = 0.3510; n = 15-22 per group). (*D*) Following isoproterenol challenge, there was a significant interaction between the effects of genotype and treatment ($F_{1,33}$ = 4.207, P = 0.0483; n = 7-11 per group). When treated with 1 mg/kg pisiferic acid, the number of hindfoot missteps in *Kcna1*$^{E283K/+}$ mice is significantly reduced compared to vehicle treatment (P = 0.025). Cartoon images created using Biorender.com.

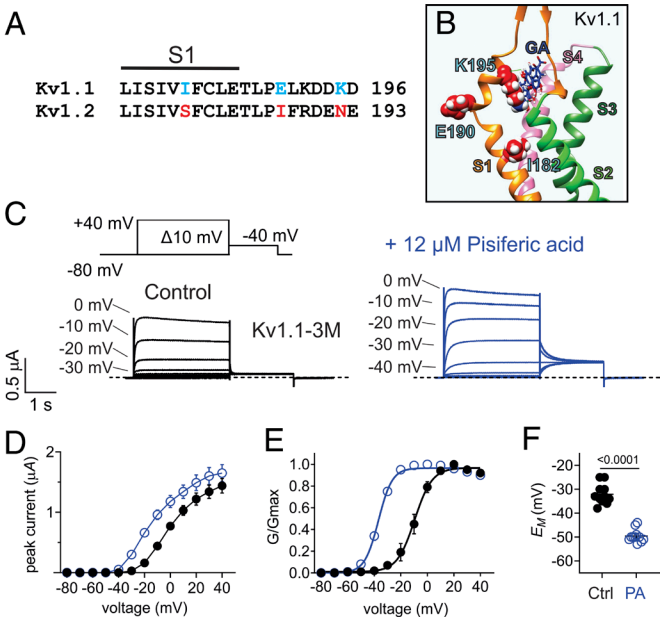

Fig. 6. Pisiferic acid does not require the gallic acid binding site for its effects on Kv1.1. Error bars indicate SEM. *n* indicates number of biologically independent oocytes. At least 2 batches of oocytes were used per experiment. Statistical comparisons by the two-tailed paired *t* test. (*A*) Sequence alignment of human Kv1.1 and Kv1.2 partial S1 and S1-S2 linker with notable Kv1.2-specific sequence differences colored (cyan versus red). (*B*) SwissDock results for unbiased docking of gallic acid (GA; blue) to the AlphaFold-predicted structure of Kv1.1. VSD helices are individually labeled and colored. Previously reported in ref. 11. (*C*) Mean traces for Kv1.1-I182S,E192I,K195N (Kv1.1-3M) channels expressed in oocytes in the absence (Control) or presence of pisiferic acid (12 μM). Scale bars *Lower Left*; voltage protocol *Upper Inset*; *n* = 11 per group. (*D*) Mean peak current (measured during prepulse) from traces as in (*C*); *n* = 11 per group. (*E*) Mean normalized tail current (G/Gmax) versus prepulse voltage for traces as in (*C*), in the absence or presence of pisiferic acid (12 μM); *n* = 11 per group. (*F*) Mean unclamped oocyte membrane potential for oocytes as in (*C*); *n* = 11 per group. PA, pisiferic acid (12 μM).

of an applied electric field. System electrostatics were quantified using particle mesh Ewald summation, which confirmed that the potential difference between the intracellular and extracellular regions was −80 mV (*SI Appendix*, Fig. S10), similar to physiological conditions at rest. Alignment of the VSDs revealed relatively small shifts in the Kv1.1 VSD conformation between the original AlphaFold2-predicted structure and that predicted by the MD simulations in the presence of the applied electric field (*SI Appendix*, Fig. S11), and conformational differences were especially minimal in the predicted location of the pisiferic acid binding site. This suggests that pisiferic acid can bind similarly to the resting conformation of Kv1.1.

Conformational Changes in the Kv1.1 VSD Induced by Ligand Binding. To examine the conformational changes that occur in the VSD upon pisiferic acid binding, we aligned the initial (apo) structure of the VSD prior to binding, to the pisiferic acid bound conformation of the Kv1.1 VSD detected in our simulations (Fig. 9 *A* and *B*). Surprisingly, comparison of the pisiferic-acid bound VSD to that of the apo, unbound VSD, revealed large-scale conformational shifts similar to that found during the activation of voltage-gated potassium channels in structural and electrophysiological studies (43, 44). Alignment of the bound-state of the Kv1.1 VSD identified in our MD simulations with that of the apo conformation indicated that pisiferic acid binding induces an upward rotation of the S3 and S4 helices about residues R295 and L296 that interact with the base of the ligand to form contacts between the S1 and S2 helices. These upward shifts in the S3 and S4 helices also caused rotations in the S4-S5 linker toward the VSD that creates tension on the pore-forming helices to trigger opening of the channel. These conformational changes suggest that the mechanism by which pisiferic acid binding increases channel activity is by altering the conformation of the channel toward an open state.

Ligand Density Maps Reveal Residue-Specific Interactions. To characterize the protein–ligand interactions responsible for binding, we computed the spatial distribution occupied by the ligand during the dynamical simulations or in other words a 3D map of the ligand density. Contouring the density at 26% revealed two high probability sites of interaction with pisiferic acid and Kv1.1 at the VSD, corresponding to the binding site detected in our MD simulations (Fig. 10*A*). A third interaction site was also detected in the pore domain, reflecting transient interactions with Kv1.1 and the ligand that are more similar to that of channel blockers. At higher probability contours density at this third site disappears, suggesting that while pisiferic acid may have some lower affinity at that interaction site, it is not the primary binding site for the ligand. We also computed the percentage of simulated time which any residue on Kv1.1 spent in contact with the pisiferic acid (e.g., residence time) (Fig. 10*B*), which showed that the highest probability contact between Kv1.1 and the ligand occurred at binding pocket residues proximal to R295, K193, and E187.

To experimentally validate the MD simulations, we tested the pisiferic acid responsiveness of Kv1.1 channels bearing single, double, and triple mutations in the residues predicted to form the pisiferic acid binding site. Consistent with the MD simulations and predicted binding pose, single or double mutations to create perturbations to the binding pocket at residues K193, E187, and R295 substantially decreased the midpoint voltage dependence of activation shift, $\Delta V_{0.5act}$, by pisiferic acid, indicative of a reduced effect and binding of pisiferic acid on Kv1.1. The triple mutant was nonfunctional (Fig. 10 *C*–*E*).

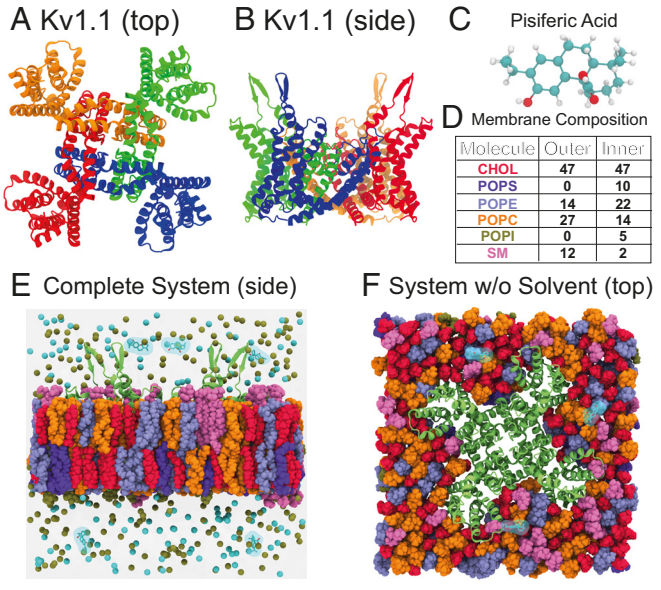

Fig. 7. All-atom molecular dynamics of the Kv1.1 ion channel. (*A*) *Top* view of a model of the Kv1.1 tetramer constructed using AlphaFold and alignment to the X-ray crystallographic structure of Kv1.2 (PDB ID: 2A79). (*B*) *Side* view of the same complex. (*C*) A ball-and-stick representation of a single pisiferic acid molecule. (*D*) The lipid composition of an asymmetric lipid bilayer found in neurons. Values in the table express the concentration of each component in terms of percentage of the total number of molecules in each layer, which corresponds to a mixture of 94 CHOL, 28 POPE, 54 POPC, and 24 SM molecules in the upper leaflet and 94 CHOL, 20 POPS, 44 POPE, 28 POPC, 10 POPI, and 4 SM molecules in the lower leaflet. (*E*) *Side* view of Kv1.1 channel embedded in the lipid membrane with 5 molecules of pisiferic acid and 150 mM KCl. Lipids are colored as in (*D*). (*F*) *Top* view of Kv1.1 embedded in an asymmetric lipid bilayer found in neurons with lipid species colored as in (*D*).

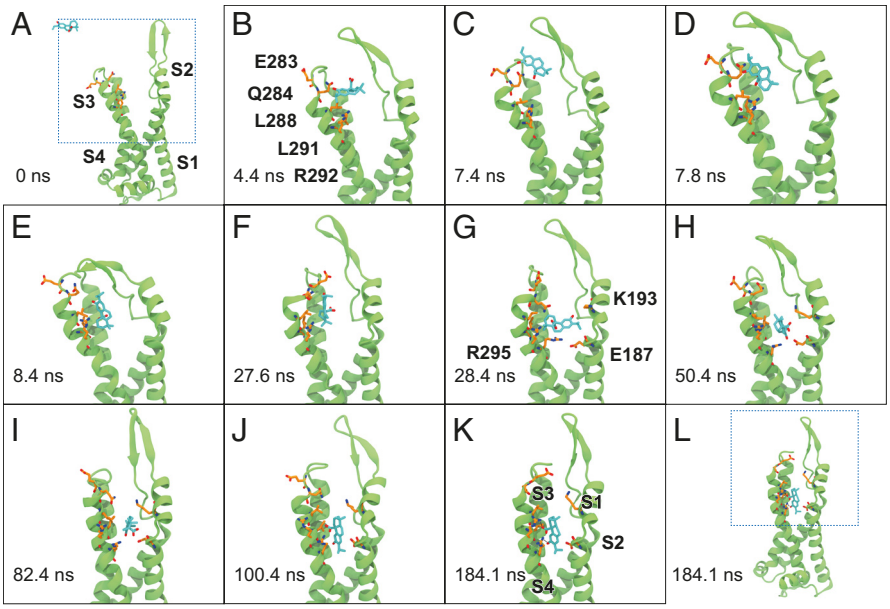

Fig. 8. MD simulations reveal the mechanism of pisiferic acid binding to the VSD of Kv1.1. (*A*) Expanded view of the S1–S4 helices and pisiferic acid in bulk solvent. Dashed lines correspond to the area in (*B*). (*B*) Close-up view of pisiferic acid. The ligand contacts and interacts with E283 and Q284 at the S4 helix. (*C*) Pisiferic acid shifts and enters a solvent-exposed cavity in the VSD. (*D*–*F*) L288, L291, and R292 coordinate the ligand as it reaches the binding pocket and (*G*) adopts a metastable configuration coordinated by K193, R295, and E187. (*H* and *I*) The ligand flips prior to settling in the stably bound pose (*J*), and remains in this conformation for the remainder of the simulation (*K*). (*L*) Expanded view of the ligand bound to the VSD.

Discussion

Aberrant function of voltage-gated potassium channels underlies a variety of inherited, de novo genetic, and/or acquired electrical excitability disorders, including Long QT syndromes 1, 2, 5, and 6 (45), Brugada syndrome (46), KCNQ2 developmental and epileptic encephalopathy (DEE) (47), KCNB1-linked DEE (48), and EA1 (1, 3). These genetic traits are generally relatively rare, but nonetheless often devastating. Episodic ataxias occur at an estimated frequency of 26/100,000 people worldwide (10), and of the nine distinct genetic forms, EA1 (caused by *KCNA1* sequence variants) and EA2 (*CACNA1A*) are the most commonly diagnosed (49, 50).

EA1 is typically treated with varying success by altering electrical excitability using the sodium channel inhibitor carbamazepine, or less commonly the carbonic anhydrase inhibitor acetazolamide, which is more often given to individuals with EA2. Attempts to directly fix the function of Kv1.1 channels carrying EA1 sequence variants have been slowed historically by limited impact of WT Kv1.1 openers on channels carrying EA1 mutations. The first reported Kv1.1 channel opener, pimaric acid, augments WT Kv1.1 currents up to eightfold (at −50 mV) at 10 μM, but at greater concentrations was found to inhibit Kv1.1, just as we observe for pisiferic acid at 100 μM (Fig. 3*C* and *SI Appendix*, Fig. S2) and also similar to niflumic acid (31). It is possible that pimaric acid is able to rescue function in Kv1.1 channels carrying EA1-linked sequence variants, but that has not to our knowledge been reported (51). We previously found that several synthetic glycine derivatives could increase WT Kv1.1 activity as much as 30-fold at submicromolar concentrations. The derivatives had the advantage of not inhibiting Kv1.1 at higher concentrations, and were at least semispecific among Kv isoforms, but, crucially, they failed to rescue the EA1 variant-containing Kv1.1 channels that we analyzed (E283K, G311D, L328V, and V408A) (52). Subsequently, as described above, we found that gallic and tannic acid, present in several extracts (bladderwrack kelp, common nettle, and Pacific ninebark) used by the Southern Kwakwaka'wakw First Nation to treat locomotor ataxia (11), open WT Kv1.1 and rescue 2/5 EA1 mutants we tested. Niflumic acid was then found to rescue one EA1 mutant Kv1.1 channel in vitro and in vivo, albeit at lower potency than pisiferic acid (31).

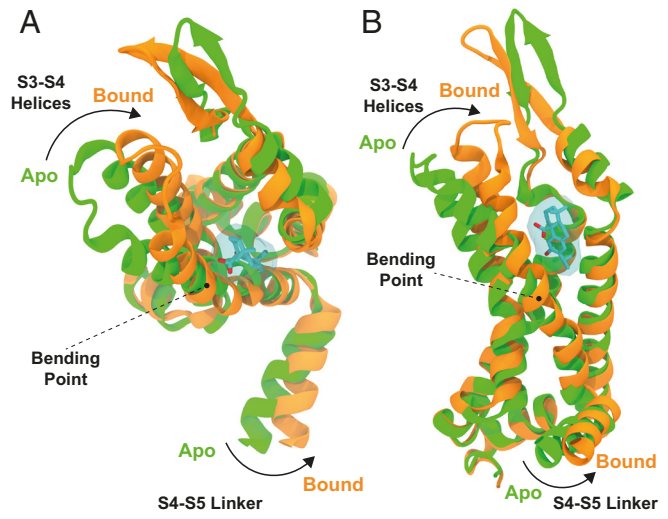

Fig. 9. Comparison of the conformational changes in Kv1.1 upon ligand binding. (*A*) *Top* view of the VSD prior (green) and after pisiferic acid stably binds (orange). The bound conformation was measured after 184 ns of MD simulations. (*B*) *Side* view of the apo Kv1.1 VSD and bound Kv1.1 VSD. Pisiferic acid binding to the VSD of Kv1.1 induces a conformational change in the S3 and S4 helices. Rotation of the S3 and S4 helices applies a torque to the S4-S5 linker, creating tension on the pore-forming helices.

One question that arises is whether pisiferic acid is able to truly rescue EA1 mutant Kv1.1 channels, or instead simply increases the current through non-mutant-interacting WT Kv1.1 channels. Our data suggest true mutant rescue, as follows. First, we found that the function of half of the 12 mutants we tested was augmented by pisiferic acid for mutant Kv1.1 channels in their homomeric, homozygous form (*SI Appendix*, Fig. S4) demonstrating unequivocally that for these mutants at least, pisiferic acid genuinely rescues the mutant form (there were no WT subunits present). We next tested heterozygous, homomeric mutant Kv1.1 currents, and found that activity of 11/12 of them was improved by pisiferic acid. The majority of these channels exhibited depolarized voltage dependence of activation compared to WT, some by >20 mV, i.e., they form channels with distinct properties to those of all-WT channels recorded in the same batches, supporting the conclusion that for the majority of cases, there are mutant subunits in the channels being rescued. In addition, pisiferic acid has notably differing magnitudes of effects (2 through 10, in terms of current fold-increase) depending on the homomeric, heterozygous Kv1.1

mutant current being studied (*SI Appendix*, Fig. S5*F*). This would not be the case if pisiferic acid were simply acting on WT channels and the mutant subunits were somehow left behind—the fold-increases would be much more uniform and similar to that of WT. We observed similar phenomena for different heteromeric, heterozygous mutant Kv1.1/Kv1.2 currents, i.e., a differing shift in voltage dependence of activation versus WT at baseline (Fig. 4*F*) and different fold-increase in current in response to pisiferic acid (Fig. 4*E*). We therefore conclude that pisiferic acid is able to restore/augment activity in the majority of channels that include EA1-linked mutant Kv1.1 subunits.

Herein, we again learned from Native American folk medicine, which involved use of conifer extracts for excitability disorders including weakness and paralysis, although our eventual lead extract was from a Japanese conifer, because of a more favorable activity profile in vitro (Fig. 2). While gallic acid interacted with the S1-S2 linker to open Kv1.1 channels (Fig. 6) (11), pisiferic acid sits much deeper in the VSD cleft, and in MD simulations was found to spontaneously bind there, following transient interactions on the way to this deep pocket (Fig. 8). The results of the MD simulations are consistent with pisiferic acid binding inducing a conformational shift in the VSD that triggers pore opening, meaning that in this context Kv1.1 is acting similarly to a classic ligand-gated channel, i.e., binding of a ligand to a protein domain on the channel's extracellular side that is distinct from but connected to the pore region leads to a ligand-induced conformational shift that opens the pore. Alternatively, this behavior can be likened to calcium-activated K^+ channels such as BK, which is

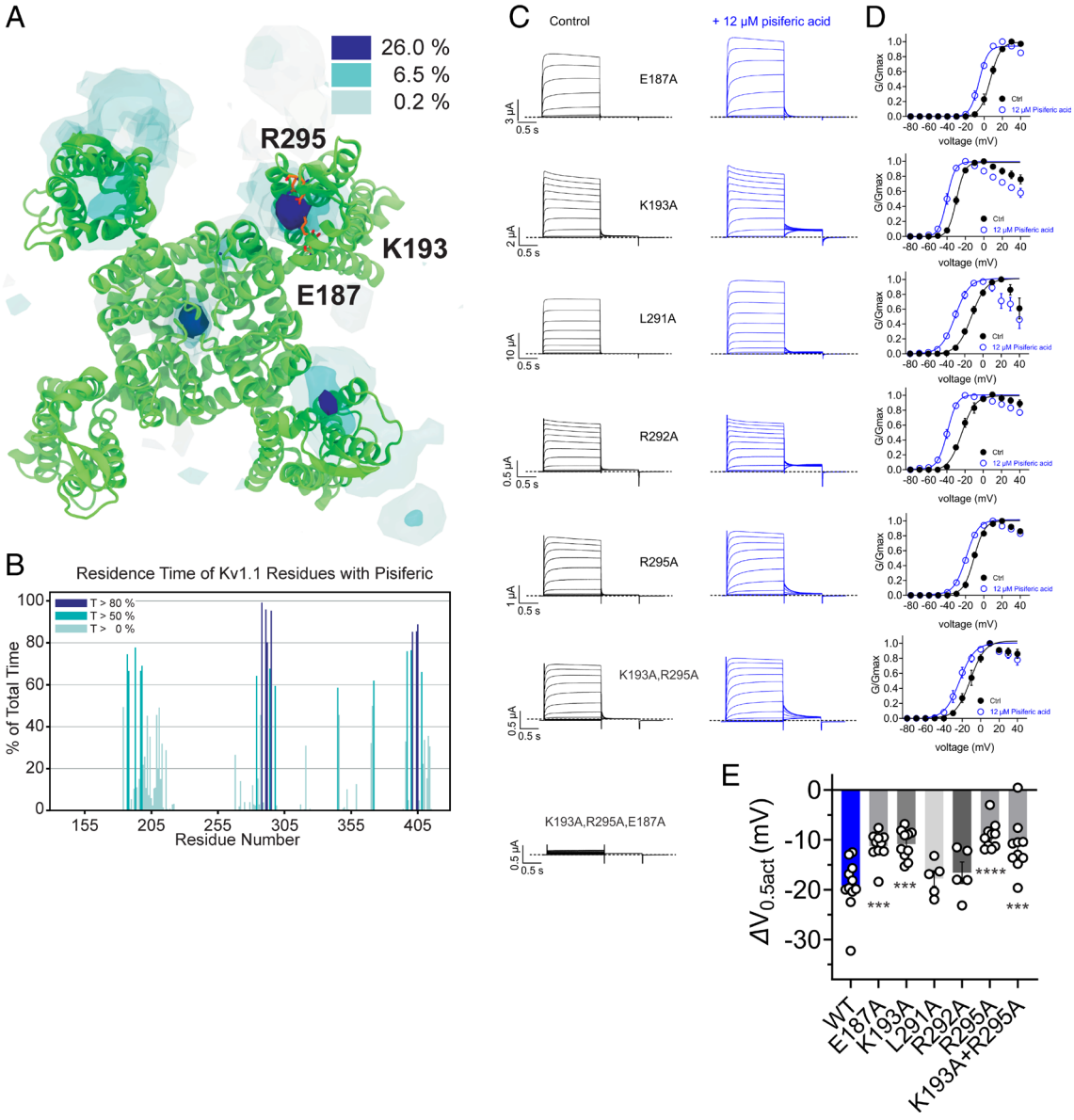

Fig. 10. Ligand density maps, residence time calculations, and experimental validation of MD simulations of pisiferic acid binding to Kv1.1. (*A*) The ligand density map highlights positions occupied by pisiferic acid during dynamical simulation. Three distinct isocontours are shown corresponding to 26, 6.5, and 0.2% occupancy in dark blue, blue, and light blue, respectively. Binding pocket residues, R295, K193, and E187 that stably interact with the ligand in the VSD are also highlighted. (*B*) Residue-specific contacts between Kv1.1 and pisiferic acid measured throughout the simulation as a percentage of time show the highest peaks in residues proximal to the VSD binding pocket (R295, E187, and K193). (*C*) Mean traces for the Kv1.1 mutants indicated expressed in oocytes in the absence (Control) or presence of pisiferic acid (12 µM). Scale bars *Lower Left*; voltage protocol as in Fig. 1*C*; n = 5-11 per group. For all electrophysiology in this figure: error bars indicate SEM. n indicates number of biologically independent oocytes. At least 2 batches of oocytes were used per experiment. Statistical comparisons by the two-tailed paired t test. (*D*) Mean normalized tail current (G/Gmax) versus prepulse voltage for traces as in (*C*), in the absence or presence of pisiferic acid (12 µM); n = 5-11 per group. (*E*) Summary of $V_{0.5act}$ shifts in response to pisiferic acid (12 µM), quantified from data in (*C* and *D*), n = 5-11. ***P < 0.001; ****P < 0.0001.

independently activated by both voltage and calcium, albeit the calcium-binding site is intracellular (53). Similar to this model, increasing pisiferic acid concentration at a fixed voltage increases the proportion of open channels, while increasing voltage at a fixed pisiferic acid concentration does the same.

A potential limitation of our study is that the cellular electrophysiology was performed using *Xenopus* oocytes rather than a mammalian expression system. However, the advantage of oocytes that we consider very important when studying heterozygote-mimics and heteromeric channels is that one injects each oocyte with relatively precise quantities of each cRNA (channel isoform, mutant) being studied, so the quantity and ratio of the cRNAs is controllable in each individual cell, which is not the case for transient transfections in mammalian cells.

Native Americans have used an estimated 3,000 plant species as medicine (12), a number that may be an underestimate given that they generally lacked their own written records, instead passing down medicinal knowledge by word of mouth. This tradition was especially prone to disruption by European colonists as they destroyed First Nations' cultures along with their people. Given that extant documentation and knowledge of Native America traditional medicines for ataxia is therefore rare for the above reasons and because of the relative rarity of inherited ataxias, we hypothesized that Native American traditional medicines for disorders that can also stem from hyperexcitability, such as pain, weakness, paralysis, and cardiovascular dysfunction, might yield clues to potential ataxia therapies. In Moerman's Native American Ethnobotany database (54), there are >30 examples of plants being used to treat paralysis, attributed to 18 different First Nations; 110 examples for weakness, >1,500 for pain; the relative frequencies of these three likely reflect the relative frequency of the disorders themselves.

Of the species we tested here, a compound decoction made by boiling *P. contorta* needle tips in water was taken orally by the Carrier First Nation, of what is now termed British Columbia, for paralysis, weakness, pain, and sores (55), and by the Thompson (as a salve of boiled sap and grease), Haisla and Hanaksiala First Nations for pain (56). A compound containing warmed *T. mertensiana* seeds was taken by the Tingit First Nation for toothache (57) and the Bella Coola applied a poultice of chewed *T. mertensiana* leaves as a burn dressing (55). *P. ponderosa* pitch was applied topically by the Flathead and Thompson to treat pain (58, 59). Extracts of all these species had interesting and potentially beneficial effects on Kv1.1 activity and warrant future study, despite us selecting a different species for further work here. Strikingly, there are to our knowledge no recorded uses of *P. albicaulis* as medicine (12, 54), and it was instead used as food; this is significant because it was the only conifer extract that did not hyperpolarize the Kv1.1 $V_{0.5act}$ (Fig. 1). We are not aware of documented use of *C. pisifera* in traditional medicine in Japan, but the extract has previously reported antibacterial properties (29). Pisiferic acid, the active component in *C. pisifera*, is also a component of rosemary (*Salvia rosmarinus*), a plant used in traditional medicine to treat neurological disorders (30).

In summary, by learning and extrapolating from Native American traditional medicine use of conifers, we have found that the Sawara cypress metabolite pisiferic acid is a uniquely versatile, potent, and efficacious Kv1.1 opener with the capability of universal correction of EA1-linked Kv1.1 mutant channels. The results of our experiments and MD simulations support a model in which Kv1.1 has the capability of functioning as a ligand-gated channel with its VSD acting as the ligand-binding domain, to which pisiferic acid binds to induce channel opening. Our findings warrant further investigation of the therapeutic potential of pisiferic acid in ataxia, in additional preclinical studies, and if supported by further data, clinical trials. Our work also further underscores the importance of preserving botanical folk medicine practices and the habitats in which medicinal plants grow. Future drugs undoubtedly lie deep in the heart of Amazonian rain forests and among tropical coral reefs but can also be hiding in plain sight among the herbs and trees in gardens, forests, chaparral, and deserts closer to home. In all these cases, realization of the potential of medicines from our natural environment requires protection of these habitats from climate change, unsustainable logging and farming practices, pollution, and other existential threats to plant and animal life.

Methods Summary

Complete methods are included in *SI Appendix*.

Plant Extracts, Electrophysiology, and MD Simulations. Briefly, methanolic extract of conifers, including those collected under permit from Yosemite National Park (study # YOSE-00839); and *C. pisifera* metabolite pisiferic acid (presence in extract confirmed by HPLC and LC/MS), were tested for effects on Kv channel heterologous expressed in *Xenopus laevis* oocytes using two-electrode voltage-clamp electrophysiology. An atomic model for Kv1.1 was constructed from the predicted structure of the Kv1.1 monomer available in the AlphaFold database (37) (UNIPROT: AF-Q09470-F1). The transmembrane segments of Kv1.1 including the S1–S6 helices were retained, and the disordered intracellular regions (residues 1 to 142 and 416 to 495) were removed from the model. An X-ray crystallographic structure for the Kv1.2 tetramer (PDB ID: 2A79) (38) was used as a template to obtain the quaternary protein–protein contacts that stabilize the Kv1.1 tetramer. MD simulations of pisiferic acid binding to Kv1.1 were conducted, and then validated using TEVC and site-directed mutagenesis.

Mouse Studies. For mouse studies, pisiferic acid (Combi-Blocks, San Diego, CA) was solubilized at 0.1 mg/mL in a vehicle containing 1% DMSO in sterile PBS. Isoproterenol hydrochloride (Sigma-Aldrich, St. Louis, MO) was made up at 0.5 mg/mL free base in sterile PBS. All compounds were injected intraperitoneally at 10 mL/kg. The *Kv1.1*-E283K transgenic mouse line was created from C57BL/6 mice by CRISPR knock-in at the Chao Family Comprehensive Cancer Center Transgenic Mouse Facility at UCI. Experimental mice were bred by crossing Kv1.1$^{E283K/+}$ mice with WT Kv1.1 mice (*Kv1.1*$^{+/+}$). The offspring were genotyped by qPCR and approximated typical Mendelian inheritance. *Kv1.1*$^{E283K/+}$ and littermate *Kv1.1*$^{+/+}$ transgenic mice were group-housed under a 12-h light/dark cycle with access to food and water ad libitum. Unless otherwise noted, all of the behavioral experiments were conducted on adult, male mice between 2 and 4 mo of age with the genotypes being tested in a counterbalanced fashion. These behavioral paradigms were approved by the Institutional Animal Care and Use Committee at the University of California, Irvine.

Statistics and Reproducibility. All values are expressed as mean ± SEM. Multiple comparison statistics were conducted using either a One-way ANOVA with a post hoc Dunnet correction for multiple comparisons or a Two-way ANOVA with a post hoc Bonferroni correction. Comparison of two groups was conducted using a *t* test; all *P* values were two-sided.

Data, Materials, and Software Availability. Raw data have been deposited in Dryad (https://doi.org/10.5061/dryad.hmgqnk9tq) (60).

ACKNOWLEDGMENTS. This study was supported by the NIH, National Institute of General Medical Sciences (GM130377) and a Samueli Scholarship (Susan Samueli Integrative Health Institute, UC Irvine) to G.W.A., and the NIH, National Institute of Allergy and Infectious Diseases (AI167034) to A.Y. We acknowledge the support of the Chao Family Comprehensive Cancer Center Transgenic Mouse Facility Shared Resource, supported by the National Cancer Institute of the NIH under award number P30CA062203. This work used Stampede3 at the Texas Advanced Computing Center through allocation (BIO230061) from the Advanced Cyberinfraction Coordination Ecosystem: Services & Support program, which is supported by the NSF, and the High Performance Community Computing Cluster at UC Irvine. The content is solely the responsibility of the authors and does not necessarily represent the official views of the NIH.

1. D. L. Browne *et al.*, Episodic ataxia/myokymia syndrome is associated with point mutations in the human potassium channel gene, KCNA1. *Nat. Genet.* **8**, 136–140 (1994), 10.1038/ng1094-136.
2. J. L. Steckley, G. C. Ebers, M. Z. Cader, R. S. McLachlan, An autosomal dominant disorder with episodic ataxia, vertigo, and tinnitus. *Neurology* **57**, 1499–1502 (2001), 10.1212/wnl.57.8.1499.
3. S. M. Hasan, M. C. D'Adamo, "Episodic Ataxia Type 1" in *GeneReviews[(R)]*, M. P. Adam *et al.*, Eds. (University of Washington, Seattle, WA, 1993).
4. P. Zerr, J. P. Adelman, J. Maylie, Characterization of three episodic ataxia mutations in the human Kv1.1 potassium channel. *FEBS Lett.* **431**, 461–464 (1998), 10.1016/s0014-5793(98)00814-x.
5. P. Zerr, J. P. Adelman, J. Maylie, Episodic ataxia mutations in Kv1.1 alter potassium channel function by dominant negative effects or haploinsufficiency. *J. Neurosci.* **18**, 2842–2848 (1998), 10.1523/JNEUROSCI.18-08-02842.1998.
6. M. C. D'Adamo *et al.*, New insights into the pathogenesis and therapeutics of episodic ataxia type 1. *Front. Cell. Neurosci.* **9**, 317 (2015), 10.3389/fncel.2015.00317.
7. K. P. Bhatia, Familial (idiopathic) paroxysmal dyskinesias: An update. *Semin. Neurol.* **21**, 69–74 (2001), 10.1055/s-2001-13121.
8. T. Brandt, M. Strupp, Episodic ataxia type 1 and 2 (familial periodic ataxia/vertigo). *Audiol. Neurootol.* **2**, 373–383 (1997), 10.1159/000259262.
9. L. Calandriello *et al.*, Acetazolamide-responsive episodic ataxia in an Italian family refines gene mapping on chromosome 19p13. *Brain* **120**, 805–812 (1997), 10.1093/brain/120.5.805.
10. M. S. Salman, Epidemiology of cerebellar diseases and therapeutic approaches. *Cerebellum* **17**, 4–11 (2018), 10.1007/s12311-017-0885-2.
11. R. W. Manville, J. Alfredo Freites, R. Sidlow, D. J. Tobias, G. W. Abbott, Native American ataxia medicines rescue ataxia-linked mutant potassium channel activity via binding to the voltage sensing domain. *Nat. Commun.* **14**, 3281 (2023), 10.1038/s41467-023-38834-6.
12. D. E. Moerman, *Native American Medicinal Plants–An Ethnobotanical Dictionary* (Timber Press, 2009).
13. G. W. Abbott, KCNQs: Ligand- and voltage-gated potassium channels. *Front. Physiol.* **11**, 583 (2020), 10.3389/fphys.2020.00583.
14. J. H. Heeroma *et al.*, Episodic ataxia type 1 mutations differentially affect neuronal excitability and transmitter release. *Dis. Model. Mech.* **2**, 612–619 (2009), 10.1242/dmm.003582.
15. H. Wang *et al.*, Zidovudine and dideoxynucleosides deplete wild-type mitochondrial DNA levels and increase deleted mitochondrial DNA levels in cultured Kearns-Sayre syndrome fibroblasts. *Biochim. Biophys. Acta* **1316**, 51–59 (1996).
16. A. Al-Sabi *et al.*, Development of a selective inhibitor for Kv1.1 channels prevalent in demyelinated nerves. *Bioorg. Chem.* **100**, 103918 (2020), 10.1016/j.bioorg.2020.103918.
17. P. D. Dodson, M. C. Barker, I. D. Forsythe, Two heteromeric Kv1 potassium channels differentially regulate action potential firing. *J. Neurosci.* **22**, 6953–6961 (2002), 10.1523/JNEUROSCI.22-16-06953.2002.
18. P. Imbrici *et al.*, A novel KCNA1 mutation in a patient with paroxysmal ataxia, myokymia, painful contractures and metabolic dysfunctions. *Mol. Cell. Neurosci.* **83**, 6–12 (2017), 10.1016/j.mcn.2017.06.006.
19. E. J. Arroyo, S. S. Scherer, On the molecular architecture of myelinated fibers. *Histochem. Cell Biol.* **113**, 1–18 (2000), 10.1007/s004180050001.
20. M. C. D'Adamo, P. Imbrici, F. Sponcichetti, M. Pessia, Mutations in the KCNA1 gene associated with episodic ataxia type-1 syndrome impair heteromeric voltage-gated K(+) channel function. *FASEB J.* **13**, 1335–1345 (1999), 10.1096/fasebj.13.11.1335.
21. J. A. Feria Pliego, C. M. Pedroarena, Kv1 potassium channels control action potential firing of putative GABAergic deep cerebellar nuclear neurons. *Sci. Rep.* **10**, 6954 (2020), 10.1038/s41598-020-63583-7.
22. D. Pinatel, C. Faivre-Sarrailh, Assembly and function of the juxtaparanodal Kv1 complex in health and disease. *Life (Basel)* **11**, 8 (2020), 10.3390/life11010008.
23. A. F. Lagalante, M. E. Montgomery, F. C. Calvosa, M. N. Mirzabeigi, Characterization of terpenoid volatiles from cultivars of eastern hemlock (Tsuga canadensis). *J. Agric. Food Chem.* **55**, 10850–10856 (2007), 10.1021/jf071947o.
24. M. Mullin *et al.*, Primary and secondary metabolite profiles of lodgepole pine trees change with elevation, but not with latitude. *J. Chem. Ecol.* **47**, 280–293 (2021), 10.1007/s10886-021-01249-y.
25. L. S. Bullington, Y. Lekberg, R. Sniezko, B. Larkin, The influence of genetics, defensive chemistry and the fungal microbiome on disease outcome in whitebark pine trees. *Mol. Plant Pathol.* **19**, 1847–1858 (2018), 10.1111/mpp.12663.
26. H. Fukui, K. Koshimizu, H. Egawa, A new diterpene with antimicrobial activity from Chamaecyparis pisifera. *Agric. Biol. Chem.* **42**, 1419–1423 (1978).
27. M. Himejima, K. R. Hobson, T. Otsuka, D. L. Wood, I. Kubo, Antimicrobial terpenes from oleoresin of ponderosa pine treePinus ponderosa: A defense mechanism against microbial invasion. *J. Chem. Ecol.* **18**, 1809–1818 (1992), 10.1007/BF02751105.
28. K. D. Welch *et al.*, A comparison of the metabolism of the abortifacient compounds from Ponderosa pine needles in conditioned versus naive cattle. *J. Anim. Sci.* **90**, 4611–4617 (2012), 10.2527/jas.2012-5232.
29. D. Xiao *et al.*, Studies on constituents from Chamaecyparis pisifera and antibacterial activity of diterpenes. *Chem. Pharm. Bull. (Tokyo)* **49**, 1479–1481 (2001), 10.1248/cpb.49.1479.
30. R. W. Manville, D. Hogenkamp, G. W. Abbott, Ancient medicinal plant rosemary contains a highly efficacious and isoform-selective KCNQ potassium channel opener. *Commun. Biol.* **6**, 644 (2023), 10.1038/s42003-023-05021-8.
31. I. Servettini *et al.*, An activator of voltage-gated K(+) channels Kv1.1 as a therapeutic candidate for episodic ataxia type 1. *Proc. Natl. Acad. Sci. U.S.A.* **120**, e2207978120 (2023), 10.1073/pnas.2207978120.
32. L. Cheng, M. C. Sanguinetti, Niflumic acid alters gating of HCN2 pacemaker channels by interaction with the outer region of S4 voltage sensing domains. *Mol. Pharmacol.* **75**, 1210–1221 (2009), 10.1124/mol.108.054437.
33. L. Dai, V. Garg, M. C. Sanguinetti, Activation of Slo2.1 channels by niflumic acid. *J. Gen. Physiol.* **135**, 275–295 (2010), 10.1085/jgp.200910316.
34. D. Fernandez, J. Sargent, F. B. Sachse, M. C. Sanguinetti, Structural basis for ether-a-go-go-related gene K+ channel subtype-dependent activation by niflumic acid. *Mol. Pharmacol.* **73**, 1159–1167 (2008), 10.1124/mol.107.043505.
35. R. W. Manville, R. Sidlow, G. W. Abbott, Case report: A novel loss-of-function pathogenic variant in the KCNA1 cytoplasmic N-terminus causing carbamazepine-responsive type 1 episodic ataxia. *Front. Neurol.* **13**, 975849 (2022), 10.3389/fneur.2022.975849.
36. P. S. Herson *et al.*, A mouse model of episodic ataxia type-1. *Nat. Neurosci.* **6**, 378–383 (2003), 10.1038/nn1025.
37. J. Jumper *et al.*, Highly accurate protein structure prediction with AlphaFold. *Nature* **596**, 583–589 (2021), 10.1038/s41586-021-03819-2.
38. S. B. Long, E. B. Campbell, R. Mackinnon, Crystal structure of a mammalian voltage-dependent Shaker family K+ channel. *Science* **309**, 897–903 (2005), 10.1126/science.1116269.
39. A. Yu, A. Y. Lau, Energetics of glutamate binding to an ionotropic glutamate receptor. *J. Phys. Chem. B* **121**, 10436–10442 (2017), 10.1021/acs.jpcb.7b06862.
40. A. Yu, A. Y. Lau, Glutamate and glycine binding to the NMDA receptor. *Structure* **26**, 1035–1043.e2 (2018), 10.1016/j.str.2018.05.004.
41. A. Yu, E. M. Y. Lee, J. Jin, G. A. Voth, Atomic-scale characterization of mature HIV-1 capsid stabilization by inositol hexakisphosphate (IP(6)). *Sci. Adv.* **6**, eabc6465 (2020), 10.1126/sciadv.abc6465.
42. A. Yu, H. Salazar, A. J. R. Plested, A. Y. Lau, Neurotransmitter funneling optimizes glutamate receptor kinetics. *Neuron* **97**, 139–149.e4 (2018), 10.1016/j.neuron.2017.11.024.
43. A. V. Grizel, G. S. Glukhov, O. S. Sokolova, Mechanisms of activation of voltage-gated potassium channels. *Acta Naturae* **6**, 10–26 (2014).
44. D. M. Kim, C. M. Nimigean, Voltage-gated potassium channels: A structural examination of selectivity and gating. *Cold Spring Harb. Perspect. Biol.* **8**, a029231 (2016), 10.1101/cshperspect.a029231.
45. A. Anantharam, S. M. Markowitz, G. W. Abbott, Pharmacogenetic considerations in diseases of cardiac ion channels. *J. Pharmacol. Exp. Ther.* **307**, 831–838 (2003), 10.1124/jpet.103.054569.
46. G. W. Abbott, KCNE4 and KCNE5: K(+) channel regulation and cardiac arrhythmogenesis. *Gene* **593**, 249–260 (2016), 10.1016/j.gene.2016.07.069.
47. J. J. Millichap, E. C. Cooper, KCNQ2 potassium channel epileptic encephalopathy syndrome: Divorce of an electro-mechanical couple? *Epilepsy Curr.* **12**, 150–152 (2012), 10.5698/1535-7511-12.4.150.
48. A. Torkamani *et al.*, De novo KCNB1 mutations in epileptic encephalopathy. *Ann. Neurol.* **76**, 529–540 (2014), 10.1002/ana.24263.
49. E. Amadori *et al.*, Genetic paroxysmal neurological disorders featuring episodic ataxia and epilepsy. *Eur. J. Med. Genet.* **65**, 104450 (2022), 10.1016/j.ejmg.2022.104450.
50. N. Maksemous, H. G. Sutherland, R. A. Smith, L. M. Haupt, L. R. Griffiths, Comprehensive exonic sequencing of known ataxia genes in episodic ataxia. *Biomedicines* **8**, 134 (2020), 10.3390/biomedicines8050134.
51. K. Sakamoto *et al.*, Molecular mechanisms underlying pimaric acid-induced modulation of voltage-gated K(+) channels. *J. Pharmacol. Sci.* **133**, 223–231 (2017), 10.1016/j.jphs.2017.02.013.
52. R. W. Manville, G. W. Abbott, Isoform-selective KCNA1 potassium channel openers built from glycine. *J. Pharmacol. Exp. Ther.* **373**, 391–401 (2020), 10.1124/jpet.119.264507.
53. B. L. Moss, S. D. Silberberg, C. M. Nimigean, K. L. Magleby, Ca2+-dependent gating mechanisms for dSlo, a large-conductance Ca2+-activated K+ (BK) channel. *Biophys. J.* **76**, 3099–3117 (1999), 10.1016/S0006-3495(99)77462-X.
54. D. E. Moerman, Native American Ethnobotany Database, A Database of Foods, Drugs, Dyes and Fibers of Native American Peoples, Derived from Plants. http://naeb.brit.org/. Accessed 1 March 2024.
55. H. I. Smith, Materia medica of the Bella Coola and neighboring tribes of British Columbia. *Natl. Mus. Can. Bull.* **56**, 49–50 (1929).
56. B. D. Compton, "Upper North Wakashan and Southern Tsimshian ethnobotany: The knowledge and usage of plants and fungi among the Oweekeno, Hanaksiala (Kitlope and Kemano), Haisla (Kitamaat) and Kitasoo Peoples of the central and north coasts of British Columbia", PhD thesis, University of British Columbia, Vancouver, BC, Canada (1993).
57. A. Krause, *The Tlingit Indians* (University of Washington Press, Seattle, 1956).
58. N. J. Turner, L. C. Thompson, M. T. Thompson, A. Z. York, *Thompson Ethnobotany: Knowledge and Usage of Plants by the Thompson Indians of British Columbia, Victoria* (Royal British Columbia Museum, 1990).
59. J. Hart, *Montana Native Plants and Early Peoples, Helena* (Montana Historical Society Press, 1992).
60. R. W. Manville *et al.*, Raw data for the manuscript "A conifer metabolite corrects episodic ataxia type 1 by voltage sensor-mediated ligand activation of Kv1.1. *Proc. Natl. Acad. Sci.*" Dryad. (2025) https://doi.org/10.5061/dryad.hmgqnk9tq. Deposited 7 December 2024.